Phase diagram of Onsager crosses

Ronald Blaak and Bela M. Mulder
FOM Institute for Atomic and Molecular Physics, Kruislaan 407, 1098 SJ Amsterdam, The Netherlands
(Received 11 February 1998)

Onsager crosses are hard nonconvex bodies formed by rigidly connecting three elongated rods, equally thick but not necessarily equally long, to form perpendicular crosses. We study the phase behavior of systems of such particles, focusing on their ability to form spatially homogeneous orientationally ordered phases with a symmetry lower than that of the standard uniaxial nematic. We treat these systems in the Onsager, second virial coefficient, approximation. We apply bifurcation analysis to build up a global picture of the phase diagram, which is then refined using approximate numerical calculations. Finally, we generalize the Gaussian approximation for the nematic orientational distribution function, to deal with the more ordered phases encountered here, and compare with the results from the previous techniques to see whether it is feasible to reliably predict the phase diagrams from a computationally cheaper technique. [S1063-651X(98)01211-2]

PACS number(s): 61.30.Cz, 64.70.Md, 83.70.Jr

I. INTRODUCTION

The generic liquid crystalline phase is nematic. It is a spatially homogeneous phase in which the orientations of the nonspherical component particles are distributed in an anisotropic fashion around a preferred axis yielding a phase with uniaxial macroscopic optical anisotropy (symmetry group $D_{\infty h}$). Is it possible to have orientationally ordered, but spatially homogeneous phases with a symmetry other than that of the nematic phase? This is a question that has occupied both theorists and experimentalists since the early 1970s. The most likely candidate is thought to be the so-called biaxial nematic phase, a phase with two mutually perpendicular axes of symmetry (symmetry group D_{2h}). It is assumed that this phase could be formed either by nonspherical particles with a rectangular box-like geometry (length greater than width greater than depth) [1–6] or by an (almost) equimolar mixture of rod- and disklike particles [7–10]. Despite theoretical and computational evidence [11–13] for the possibility of its existence, to date this phase still has not been demonstrated unambiguously experimentally [14–20].

A few years ago Frenkel [21] argued that it is possible to create a phase with cubic orientational anisotropy (symmetry group O_h). To this end he suggested looking at highly nonconvex hard particles obtained by gluing together highly elongated rodlike particles to form a perpendicular cross with arms of equal length (see Fig. 1). In an approximate calculation he was able to show that the stable high-density phase of such a system indeed would have cubic orientational order, thus forming a phase that he called cubatic. Our purpose here is to ''give body'' to these predictions and discuss the phase diagram of these crosslike particles in greater detail, allowing also the lengths of the individual rods within each particle to differ. Collectively we will denote this class of particles by the name Onsager crosses. This is appropriate not only as a tribute to Onsager's seminal contributions to the theory of lyotropic liquid crystals, but also because we will argue that Onsager crosses can in fact be reliably treated within the Onsager second virial approximation [22], at least if the aspect ratio of the component rods is high enough.

The choice to model these effects in hard particle systems is one of expediency rather than principle. Hard particle models have the dual advantage of serving as reference systems to which energetic interactions can be added perturbatively as well as being directly applicable to lyotropic liquid crystals formed by sterically stabilized colloidal suspensions. Moreover the theory of hard particles in the Onsager approximation is formally identical to the mean field approach usually applied to models for thermotropic liquid crystals. At a technical level these two approaches pose similar problems and their analysis is virtually identical.

The rest of the paper is organized as follows. In Sec. II we introduce the Helmholtz free energy as a functional of the one-particle orientational distribution function and derive some basic results from the symmetries of our model. In Sec. III we will analyze the behavior of our particles in three different ways. First we will use a bifurcation analysis that gives a global idea of the phase diagram concerning the transition from an isotropic to an ordered phase. Second, we try to find numerical solutions that minimize the free energy and by analyzing the distribution functions we obtain the symmetry of the phases and find sequences of transitions. As a third method we solve the model within a Gaussian approximation, which means that we assume that the distribution functions will be sharply peaked. In Sec. IV we will summarize and combine our results obtained by the different methods. We will discuss the validity of some of our assumptions and give a few suggestions for further research. In the Appendix we collect some technical background material on the construction of symmetry-adapted functions from the standard rotation matrices and prove some of their properties that are used in the main text.

II. FORMULATION OF THE MODEL

A. Free-energy functional

In order to study our system we will need an appropriate free-energy functional. Onsager showed that at least for a fluid of very elongated rods, the excess free energy can be effectively be truncated at second virial coefficient level, yielding a theory with the formal structure of a mean-field theory. Even in the cases where the truncation is not *a priori*

justified, this approximation still contains the essential ingredients of the physics of such systems, viz., the competition between orientational and translational entropy. Though our particles are no longer the elongated rods as in Onsager's original model, they do consist of three of these kind of objects. Together, they form a very open structure. This means that the probability of multiple overlaps between two particles in general will be very small. As a consequence we might expect that the rods act independently of each other, which allows us to use reasoning similar to Onsager's and truncate the free-energy expansion in virial coefficients after the second virial coefficient. This leads to the free-energy functional

$$\beta f[\psi]=\int d\Omega\ \psi(\Omega)\ln\psi(\Omega) + \frac{1}{2}\rho\int d\Omega_1\int d\Omega_2\psi(\Omega_1)\psi(\Omega_2)\mathcal{K}(\Omega_1,\Omega_2)+\beta\hat{f}. \tag{1}$$

Here f is the free energy per particle, which is a functional of ψ the orientational distribution function (ODF). This ODF is a measure for the fraction of particles with an orientation Ω in a fixed reference frame and is normalized to unity. $\beta=(k_BT)^{-1}$, the inverse temperature.

The first term of the free-energy functional is associated with the orientational entropy of the system. The second term takes into account the interaction between the particles, described by $\mathcal{K}(\Omega_1,\Omega_2)$, the excluded volume of two particles with given orientations. The last term is the ideal gas term and does not depend on the ODF.

In general we need three parameters to describe any orientation Ω. For this we make use of the Euler angles (α,β,γ) describing an arbitrary rotation in three-dimensional space.

A necessary condition for an equilibrium ODF of a system described by a free energy functional is that it satisfies the stationarity condition

$$\frac{\delta}{\delta\psi(\Omega)}\left\{f[\psi]-\mu\int d\Omega\ \psi(\Omega)\right\}=0, \tag{2}$$

where the second term, via the Lagrange multiplier μ, takes care of the normalization of the ODF. To ensure that the solution is stable we need to check whether it is a minimum of the free energy and, in the case of phase coexistence, to equate the chemical potentials and pressures of the different phases.

B. Excluded volume

The main contribution to the excluded volume of two elongated rods with lengths L_1 and L_2 and diameters D_1 and D_2 is given by

$$v_{excl}=L_1L_2(D_1+D_2)|\sin\gamma|, \tag{3}$$

where γ is the angle between the long axis of the particles. We assume that the excluded volume of two crosses can be approximated by the sum of pairwise overlaps of the rods, which form the crosses. This assumption is based on the fact that the probability for multiple overlaps between two crosses will be small compared to that of a single overlap. As a consequence of this assumption, one is not able to make a distinction between crosses in which the rods are connected at different locations, e.g., at the ends of the rods.

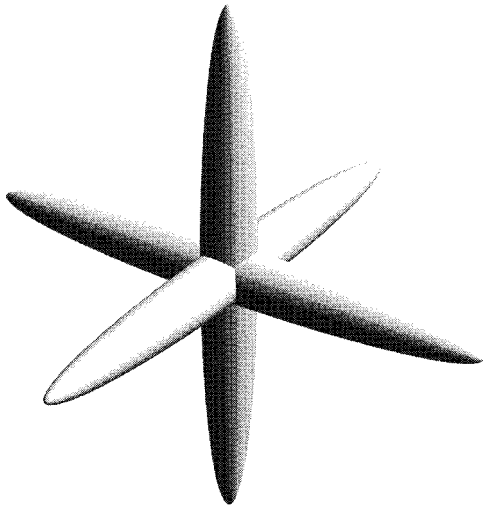

FIG. 1. Onsager cross for $L/D=10$.

If we denote the lengths of the three rods pointing respectively in the x, y, and z directions of a particle fixed frame by L_1, L_2, and L_3 and take equal diameters D for all rods, we obtain for the leading term in the excluded volume of two crosslike particles labeled with superscripts (1) and (2)

$$v_{cross}=\sum_{i,j}\ 2L_i^{(1)}L_j^{(2)}D|\sin\gamma_{ij}|=2L^2D\sum_{i,j}\ l_i^{(1)}l_j^{(2)}|\sin\gamma_{ij}|, \tag{4}$$

where $l_i=L_i/L$ and the sum of the lengths of the rods is given by $L=L_1+L_2+L_3$. γ_{ij} denotes the angle between the ith rod of particle 1 and the jth rod of particle 2. It is convenient to express the density ρ in terms of the second virial coefficient, which is half of the mean excluded volume in the isotropic phase and, using $\langle|\sin\gamma_{ij}|\rangle_I=\pi/4$, this results in

$$B_2=\frac{1}{2}\langle v_{cross}\rangle_I=\frac{\pi}{4}L^2D. \tag{5}$$

We now introduce a reduced density $\eta\equiv B_2\rho$. Since the excluded volume interaction between two particles depends only on their mutual orientation $\Omega_{12}=\Omega_2^{-1}\Omega_1$, we define the reduced excluded volume interaction by

$$\mathcal{E}(\Omega_{12})\equiv\frac{\mathcal{K}(\Omega_1,\Omega_2)}{B_2}=\frac{8}{\pi}\sum_{i,j}\ l_i^{(1)}l_j^{(2)}|\sin\gamma_{ij}|. \tag{6}$$

In general, any function of Ω can be expanded in the rotation matrix elements $\mathcal{D}^l_{m,n}(\Omega)$. (Throughout the rest of this article we will use the conventions for these functions as can be found in [23].) However, in this case it is convenient to exploit the extra symmetries in our problem in order to obtain a smaller subset of symmetry adapted functions. The particles, and therefore their interactions as well, are invariant under rotations over an angle π about any of the three axes in the particle fixed frame. Together with the identity,

these three rotations form the group $D_2=\{1,R_x(\pi),R_y(\pi),R_z(\pi)\}$. We now introduce the symmetry adapted functions

$$\Delta^l_{m,n}(\Omega)\equiv\frac{1}{\sqrt{N}}\sum_{g,g'\in D_2}\mathcal{D}^l_{m,n}(g'\Omega g^{-1}). \tag{7}$$

The normalization constant N is chosen in order to achieve the orthogonality relation

$$\int \Delta^l_{m,n}(\Omega)\Delta^{l'}_{m',n'}(\Omega)d\Omega=\frac{8\pi^2}{2l+1}\delta_{l,l'}\delta_{m,m'}\delta_{n,n'}. \tag{8}$$

If we work out the definition for these functions, we find that both indices m and n have to be even and the functions are real and are of the form

$$\Delta^l_{m,n}=\left(\frac{1}{\sqrt{2}}\right)^{2+\delta_{m,0}+\delta_{n,0}}\{\mathcal{D}^l_{m,n}+(-)^l\mathcal{D}^l_{m,-n}+(-)^l\mathcal{D}^l_{-m,n}+\mathcal{D}^l_{-m,-n}\}. \tag{9}$$

Both m and n are chosen to be non-negative. In the case of odd values for l, both indices need to be positive in order to maintain a nonzero function, as can be seen directly form this definition [24].

To give an impression what these functions look like, we list here the four that have $l=2$, discussed by Straley [3]:

$$\begin{aligned}\Delta^2_{0,0}(\Omega)&=\frac{1}{2}(3\cos^2\beta-1),\\ \Delta^2_{0,2}(\Omega)&=\frac{1}{2}\sqrt{3}\sin^2\beta\cos 2\gamma,\\ \Delta^2_{2,0}(\Omega)&=\frac{1}{2}\sqrt{3}\sin^2\beta\cos 2\alpha,\end{aligned} \tag{10}$$

$$\Delta^2_{2,2}(\Omega)=\frac{1}{2}(1+\cos^2\beta)\cos 2\alpha\cos 2\gamma-\cos\beta\sin 2\alpha\sin 2\gamma.$$

We are now able to expand the excluded volume interaction (6) in these symmetry adapted Δ functions

$$\mathcal{E}(\Omega)=\sum_{l,m,n}\frac{2l+1}{8\pi^2}E_{l,m,n}\Delta^l_{m,n}(\Omega), \tag{11}$$

where the coefficients $E_{l,m,n}$ are formally given by

$$E_{l,m,n}=\int d\Omega\mathcal{E}(\Omega)\Delta^l_{m,n}(\Omega) \tag{12}$$

and are symmetric in m and n ($E_{l,m,n}=E_{l,n,m}$) because the interaction is invariant under interchanging the particles. In order to calculate these coefficients $E_{l,m,n}$ we need to evaluate integrals of the type

$$\int d\Omega|\sin\theta_{ij}|\Delta^l_{m,n}(\Omega)=\int d\Omega|\hat{\mathbf{e}}^{(1)}_i\times\hat{\mathbf{e}}^{(2)}_j|\Delta^l_{m,n}(\Omega), \tag{13}$$

where $\hat{\mathbf{e}}^{(k)}_i$ is the unit vector pointing along the rod l_i of particle k. This can be achieved by introducing the rotations q_i about the axes of the particle fixed frame

$$\begin{aligned}q_1&=R_y(\pi/2),\\ q_2&=R_x(-\pi/2),\\ q_3&=\mathbf{1}\end{aligned} \tag{14}$$

and using them as coordinate transformations in order to redirect the rods $l^{(1)}_i$ and $l^{(2)}_j$ along the z axis, which enables us to obtain a more convenient form for the integrals (13)

$$\begin{aligned}&\int d\Omega|q_i\hat{\mathbf{e}}^{(1)}_z\times q_j\hat{\mathbf{e}}^{(2)}_z|\Delta^l_{m,n}(\Omega)\\ &=\int d\Omega|\hat{\mathbf{e}}^{(1)}_z\times\hat{\mathbf{e}}^{(2)}_z|\Delta^l_{m,n}(q_j^{-1}\Omega q_i)\\ &=\sum_{m',n'}\int d\Omega|\sin\beta|\Delta^l_{m,m'}(q_j^{-1})\Delta^l_{m',n'}(\Omega)\Delta^l_{n',n}(q_i)\\ &=\sum_{m',n'}\Delta^l_{m,m'}(q_j^{-1})\Delta^l_{n',n}(q_i)\int d\Omega|\sin\beta|\Delta^l_{m',n'}(\Omega).\end{aligned} \tag{15}$$

After performing the coordinate transformation in the first line we used the properties (A3) and (A4) of the Δ functions, which state that they form a closed set under the symmetry operations of the cubic group O.

The integral in the last line of Eq. (15) can be calculated exactly and is nonzero only for $m'=n'=0$ and even values of l (see [25] Eq. 7.132.1)

$$\begin{aligned}\mu_{2l}&=\int_0^{2\pi}d\alpha\int_0^{2\pi}d\gamma\int_0^{\pi}d\beta\sin\beta|\sin\beta|\Delta^{2l}_{0,0}(\alpha,\beta,\gamma)\\ &=(2\pi)^2\int_0^{\pi}d\beta\sin^2\beta P_{2l}(\cos\beta)\\ &=-\frac{2\pi^3}{(l+1)(2l-1)2^{4l}}\binom{2l}{l}^2,\quad \mu_{2l+1}=0.\end{aligned} \tag{16}$$

Using the property of the Δ functions for the inverse rotation (A2), this gives us the final result for the coefficients $E_{l,m,n}$,

$$E_{l,m,n}=\frac{8}{\pi}\mu_l\sum_{i,j}l_il_j\Delta^l_{0,m}(q_j)\Delta^l_{0,n}(q_i). \tag{17}$$

In Table I the values of the most important $\Delta^l_{0,n}(q_i)$ are listed.

It is convenient to introduce some shorthand notation analogous to that in [26]. We define the inner product for real functions f and g of Ω,

$$\langle f|g\rangle\equiv\int f(\Omega)g(\Omega)d\Omega. \tag{18}$$

TABLE I. The most important values of $\Delta^l_{0,n}$ as a function of the three different rotations q_i.

Δ^l_{0n}	q_1	q_2	q_3
$\Delta^2_{0,0}$	$-\frac{1}{2}$	$-\frac{1}{2}$	1
$\Delta^2_{0,2}$	$\frac{1}{2}\sqrt{3}$	$-\frac{1}{2}\sqrt{3}$	0
$\Delta^4_{0,0}$	$\frac{3}{8}$	$\frac{3}{8}$	1
$\Delta^4_{0,2}$	$-\frac{1}{4}\sqrt{5}$	$\frac{1}{4}\sqrt{5}$	0
$\Delta^4_{0,4}$	$\frac{1}{8}\sqrt{35}$	$\frac{1}{8}\sqrt{35}$	0

We can also define a functional in this space of real functions by

$$f[g](\Omega)=\int d\Omega' f(\Omega'^{-1}\Omega)g(\Omega'). \tag{19}$$

If we apply this last definition to $\mathcal{E}$ and use the fact that it depends only on relative orientations, we obtain

$$\begin{aligned}\langle f|\mathcal{E}[g]\rangle &= \int d\Omega_1 \int d\Omega_2 \mathcal{E}(\Omega_2^{-1}\Omega_1) f(\Omega_1) g(\Omega_2) \\ &= \langle \mathcal{E}[f]|g\rangle. \end{aligned} \tag{20}$$

With this notation we can write the free-energy functional (1) in a more compact form as

$$\beta f[\psi]=\langle \psi|\ln\psi\rangle+\frac{1}{2}\eta\langle\psi|\mathcal{E}[\psi]\rangle+\beta\hat{f}. \tag{21}$$

In order to understand the behavior of the excluded volume as a functional, we apply Eq. (11) to a Δ function. If we now use Eq. (A7) we immediately obtain

$$\mathcal{E}[\Delta^l_{m,n}]=\sum_p E_{l,n,p}\Delta^l_{m,p}. \tag{22}$$

This means that the total space $\mathcal{S}_\Omega$ of the $\Delta^l_{m,n}$ is decomposed into invariant subspaces $\mathcal{S}^l_m$ by the excluded volume interaction. Moreover, Eq. (22) shows that for fixed l the action of $\mathcal{E}$ is represented by the same matrix $(E_l)_{n,p}$, in all the subspaces $\mathcal{S}^l_m$ for $m=0,2,\ldots,l$.

III. ANALYSIS OF THE PROBLEM

We now return to the stationarity equation (2). With our notation we can perform the functional derivative explicitly and write it compactly as

$$\ln\psi+\eta\mathcal{E}[\psi]-\beta\mu=0, \tag{23}$$

where the ODF ψ satisfies the normalization $\langle 1|\psi\rangle=1$. Any solution that minimizes the free energy must be a solution of this equation. We assume that the ODF possesses the same symmetry D_2 as that of our particles and hence can be expanded in the Δ functions

$$\psi(\Omega)=\sum_{l,m,n}\frac{2l+1}{8\pi^2}\psi_{l,m,n}\Delta^l_{m,n}(\Omega), \tag{24}$$

with some constant coefficients $\psi_{l,m,n}$. Intuitively, this seems justified since a homogeneous phase with symmetry that is a subgroup of the symmetry group of the constituent particles seems implausible. To our knowledge, however, no rigorous proof exists for this statement. Moreover, the symmetry of the phase need not be contained in that of the particles: cut spheres, for instance, have uniaxial symmetry ($D_{\infty h}$) but can form a cubatic phase [27].

We are going to use three different methods to study the behavior of our system. First, we will use a bifurcation analysis to study the possible transitions of the isotropic phase to orientationally ordered phases. This is a fast method that gives a global description of the phase behavior and tells us some of the symmetries of the phases we might expect. However, the method has its limitations: It is possible to obtain several phases with different symmetries and the method does not tell us which is the thermodynamically most stable phase. Moreover, it disregards the possibility of a strong first-order transition to a phase that does not bifurcate from the isotropic phase.

The second method we will use is minimizing the free-energy functional by solving the stationarity condition (23) numerically. Due to the finite set of functions in which the ODF is expanded, we can only hope to do so properly if the ODF is a not too strongly peaked function. Thus the results are useful only for low densities when the phases are probably not yet strongly ordered. For higher densities, the results, though they might be an indication, are not reliable in predicting the densities for phase transitions. For these densities we will use a third method, which uses the so-called Gaussian approximation. We will assume that for higher densities the ODF becomes strongly peaked and can be approximated by a combination of Gaussians.

A. Bifurcation analysis

We used a bifurcation analysis to obtain an upper limit η_0 for the density at which the isotropic phase $\psi_0=1/8\pi^2$ becomes unstable with respect to orientational ordering. This analysis also yields the possible symmetry breaking modes, allowing a coarse picture of the phase diagram to be built. For a more detailed description we refer to Ref. [28]; here we will only indicate the main results.

We use the expansions

$$\begin{aligned}\psi&=\psi_0+\varepsilon\psi_1+\varepsilon^2\psi_2+\cdots,\\ \eta&=\eta_0+\varepsilon\eta_1+\varepsilon^2\eta_2+\cdots\end{aligned} \tag{25}$$

and the stationarity equation (23) to obtain the set of bifurcation equations of which the first is given by

$$\frac{\psi_1}{\psi_0}+\eta_0\mathcal{E}[\psi_1]=0. \tag{26}$$

Due to the special form (17), this eigenvalue problem can be solved completely. For each subspace S^l_m there is only one nonzero eigenvalue λ_l and corresponding eigenfunction χ^l_m.

The bifurcation density is given by $\eta_0=-1/\psi_0\lambda_l$, where λ_l is the negative eigenvalue with the largest absolute value.

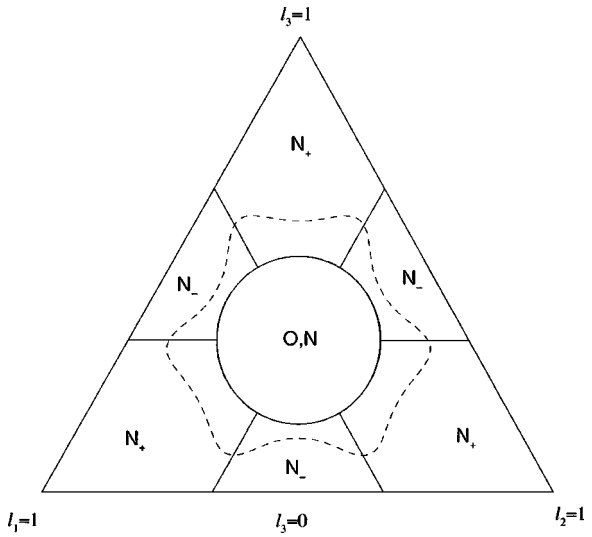

FIG. 2. Phase diagram of the phase transition at lowest density according to the bifurcation analysis. N_+ and N_- correspond to a rodlike and a disklike nematic phase, respectively, while O is used to denote the cubatic phase. The lines form the boundary between areas of rodlike and disklike behavior. Points on the dashed line have $\eta_2=0$; outside and inside η_2 has a negative and positive value, respectively.

A linear combination of corresponding eigenfunctions is used to obtain the unstable mode from the second-order bifurcation equation.

The resulting qualitative phase diagram is shown in Fig. 2. Our phase diagram has a triangular form and is that part of the plane $l_1+l_2+l_3=1$ for which $l_1,l_2,l_3\geqslant 0$, in which each point describes a specific particle. For instance, at the top of the triangle we have $l_3=1$ and $l_1=l_2=0$. This points therefore represents the particle formed by a single rod. On the other hand, the base of the triangle is a line for which $l_3=0$ and represents, except for the edges, particles effectively consisting of only two rods of nonzero length. All points inside the triangle correspond to particles with three rods. For simplicity, we have drawn only constant density planes of the phase diagram.

The two relevant eigenvalues λ_2 and λ_4, which have the same value on the circle, form the boundary between the area outside, where λ_2 dominates, and inside, where λ_4 dominates the bifurcation. λ_2 leads to a single unstable mode for the isotropic phase with a uniaxial symmetry, generically denoted by N, corresponding to a nematic phase. Inside the circle there are two unstable modes, of which one has a nematic symmetry while the other has a cubatic symmetry, which we denote by O [29].

The six straight lines connecting the edges of the triangle with the circle correspond to particles for which one of the l_i equals 1/3. They form the boundaries between the areas of the two nematic phases, which we denote by N_+ and N_-. They differ in the sense that, in the first case, the longest rods tend to align and, in the other case, the shortest rods align. On the lines the first-order term in the density expansion $\eta_1=0$. This leads to a trivial second-order bifurcation equation and we need to solve the bifurcation equation up to the fourth order to obtain the form of the unstable mode, which turns out to be identical to the one found for the N_+ region.

Since $\eta_1\neq 0$, the transition in general will be first order. Only on the lines where $\eta_1=0$ could a continuous transition be expected. For that reason, for particles outside the circle, we plotted the curve (dashed line) for which the second term η_2 in the density expansion is zero. Outside this curve η_2 is positive and η_3 turns out to be the first negative term. So if possible at all, a continuous transition will occur near the point where the lines and the boundary of the triangle meet.

B. Numerical calculations

1. Theory

We have seen that the bifurcation analysis gives us an idea of what might happen for the first phase transition. It shows possible symmetries of the phases and for which kind of particle we might expect them and also gives an upper limit to the transition densities. What it does not tell is whether the predicted transitions are real and, if they are, at which densities they occur. In this section we deal with this problem.

Density functional theory tells us that if we have found the ODF that gives the minimal free energy (1), it coincides with the equilibrium ODF and is the stable state of the system. Thus, what we ought to do is construct a trial function that is characterized by a number of parameters and determine the parameter values that minimize the free energy. Since the ODF is a probability distribution function, it is positive; hence we take the ansatz

$$\psi(\Omega)=\exp\left(\sum_{l,m,n}\psi_{l,m,n}\chi^l_{m,n}(\Omega)\right), \tag{27}$$

where we have expanded the ODF in the complete set of orthogonal eigenfunctions of the excluded volume interaction. The $\psi_{l,m,n}$ can be seen as parameters of the function ψ. We assign them starting values for fixed density and calculate the free energy. At this point we employ an iterative process to optimize the coefficients to minimize the free energy. The normalization is maintained by adjusting $\psi_{0,0,0}$.

Instead of minimizing the free energy, however, we try to find solutions of the stationarity condition (23) and check afterward if it corresponds to a minimum for the free energy. If we use our trial function, we obtain

$$\sum_{l,m,n}\psi_{l,m,n}\chi^l_{m,n}(\Omega)+\eta\mathcal{E}[\psi]=\beta\mu. \tag{28}$$

If we now multiply this equation with $\chi^l_{m,n}$, integrate over Ω, and use Eq. (20) and the orthogonality of the eigenfunctions, we obtain a set of equations

$$\frac{8\pi^2}{2l+1}\psi_{l,m,n}=-\eta\langle\chi^l_{m,n}|\mathcal{E}[\psi]\rangle=-\eta\langle\psi|\mathcal{E}[\chi^l_{m,n}]\rangle. \tag{29}$$

From this result we can conclude immediately that we only have to use those eigenfunctions χ^l_m of the excluded volume that have a nonzero eigenvalue. Hence we can rewrite our trial function (27) as

$$\psi(\Omega)=\exp\left(\sum_{l,m}\psi_{l,m}\chi_m^l(\Omega)\right), \tag{30}$$

where the coefficients $\psi_{l,m}$ have to satisfy

$$\psi_{l,m}=-\frac{2l+1}{8\pi^2}\eta\lambda_l\langle\chi_m^l|\psi\rangle \tag{31}$$

for even values of l and m where $0\leqslant m\leqslant l$ and the coefficient $\psi_{0,0}$ is determined by the normalization condition $\langle 1|\psi\rangle=1$. From these equations the coefficients can, in principle, be calculated self-consistently.

Next we identify each phase by means of a set of orientational order parameters, for which we will take the $\langle\Delta_{m,n}^l\rangle$. If there are nonzero $\langle\Delta_{m,n}^2\rangle$, we first rotate our solution for the ODF in such a way that $\langle\Delta_{0,0}^2\rangle$ has the absolute maximal value. This is done by rotating the reference frame as well as the initial orientation of the particle.

For the nematic phase, we could now take, for instance, the usual second-order Legendre polynomial as an order parameter

$$\mathcal{N}=\langle\Delta_{0,0}^2|\psi\rangle. \tag{32}$$

The problem, however, is that a nonzero nematic order parameter does not tell us whether we actually have a nematic phase because it will also be nonzero for a biaxial phase. Thus instead of determining whether a certain order parameter is nonzero, it is more useful to look for order parameters that are zero, which tell us which symmetry is not present in the system.

For the isotropic phase, we know that the ODF is a constant. This implies that all order parameters vanish or, equivalently, that if there is a nonzero order parameter, it is not an isotropic phase.

For the nematic phase, the D_4 phase and the D_2 phase there is at least one of the rods of the particles that tends to align and hence $\langle\Delta_{0,0}^2\rangle\neq 0$. However, for the cubatic phase, the ODF should be invariant under rotations over $\pi/2$ around any of the three frame axes, which means that there cannot be any terms present with $l=2$. Hence, if we find that $\langle\Delta_{m,n}^2\rangle=0$, and there are also nonzero order parameters for $l=4$, we have a cubatic phase.

If we find that $\langle\Delta_{m,n}^l\rangle\propto\delta_{0,m}$, we have a solution that is invariant under rotations around the z axis and hence a nematic phase. Furthermore, if we determine which rod is aligned best with the nematic direction, we know whether we have a rodlike or plateletlike nematic phase.

Finally, if $\langle\Delta_{2,2}^2\rangle\neq 0$, the ODF is not invariant under rotations over $\pi/2$ around the z axis, and the phase cannot be D_4; thus it has to be the D_2 phase. This leaves for the D_4 phase that $\langle\Delta_{2,2}^2\rangle=0$. In this case we can again determine the rod aligned best with the z axes and distinguish between D_{4+} and D_{4-}.

We have summarized these results in Table II, where we show which order parameters should be zero for each phase. We have chosen to use $\langle\Delta_{2,2}^2\rangle$ and $\langle\Delta_{4,4}^4\rangle$, but these choices are arbitrary as long as they possess the right symmetry.

Given a solution of the stationarity Eq. (28), we can calculate the free energy. As can be seen in Eq. (1), this involves a six-dimensional integral, but this can be avoided. Since the ODF satisfies Eq. (28), an equation in Ω, and the right-hand side is a constant, which equals $\psi_{0,0}+2\eta$, we can write the free energy as

$$\beta f=\frac{1}{2}\langle\psi|\ln\psi\rangle+\frac{1}{2}\psi_{0,0}+\eta+\beta\hat{f}. \tag{33}$$

After having checked whether the solution is indeed the minimum of the free energy, the pressure and chemical potential can easily be calculated by

$$\beta P=\rho+\rho^2B_2(\psi)=\frac{\eta}{\langle B_2\rangle_I}\left(1+\frac{1}{2}\eta\langle\psi|\mathcal{E}[\psi]\rangle\right) \tag{34}$$

and

$$\frac{\beta G}{N}=\beta f+\frac{\beta P}{\rho}=1+\psi_{0,0}+2\eta+\beta\hat{f}, \tag{35}$$

where the last term is given by $\beta\hat{f}=\ln\eta+\text{const}$. If now for different densities we find equal pressure and chemical potential, we have coexistence of different phases.

TABLE II. For each of the isotropic, nematic, cubatic D_4, and D_2 phases, it is indicated whether the four chosen order parameters are zero or nonzero. The order parameter are determined by evaluating their average weighted by the ODF ψ. For the nematic, D_4, and D_2 phases there is one preferred direction for the particles. In the case of the nematic phase the order is rotationally symmetric about that direction, while in the case of the D_4 or D_2 phase this symmetry is broken and the rotational symmetry is discrete and is four-fold or two-fold.

Phase	$\Delta_{0,0}^2$	$\Delta_{2,2}^2$	$\Delta_{0,0}^4$	$\Delta_{4,4}^4$
Isotropic	0	0	0	0
Nematic	nonzero	0	nonzero	0
Cubatic	0	0	nonzero	nonzero
D_4	nonzero	0	nonzero	nonzero
D_2	nonzero	nonzero	nonzero	nonzero

2. Numerical results

We solve the set of self-consistency equations that we derived in the preceding subsection, where we only use the functions with $l=2$ and $l=4$. By using several starting values we obtain, by means of an iterative process, different numerically stable solutions. Given a stable solution, we can calculate the free energy and check that it is a minimum.

By taking more terms into account, the coefficients change as well as the densities for which the transitions occurs. However, since we are interested only in a qualitative picture, this is of no real importance because the symmetry of the obtained phase remains the same. We used Eq. (33) to calculate the free energy and in that way avoid the six-dimensional integral. However, since we truncated the expansion of the ODF at $l=4$, this means that we also truncate the free energy. If we find solutions of the ODF with different symmetries, we use this approximated value for the free energy to determine the most stable phase. So we end up only with an estimate for the density at which the phase

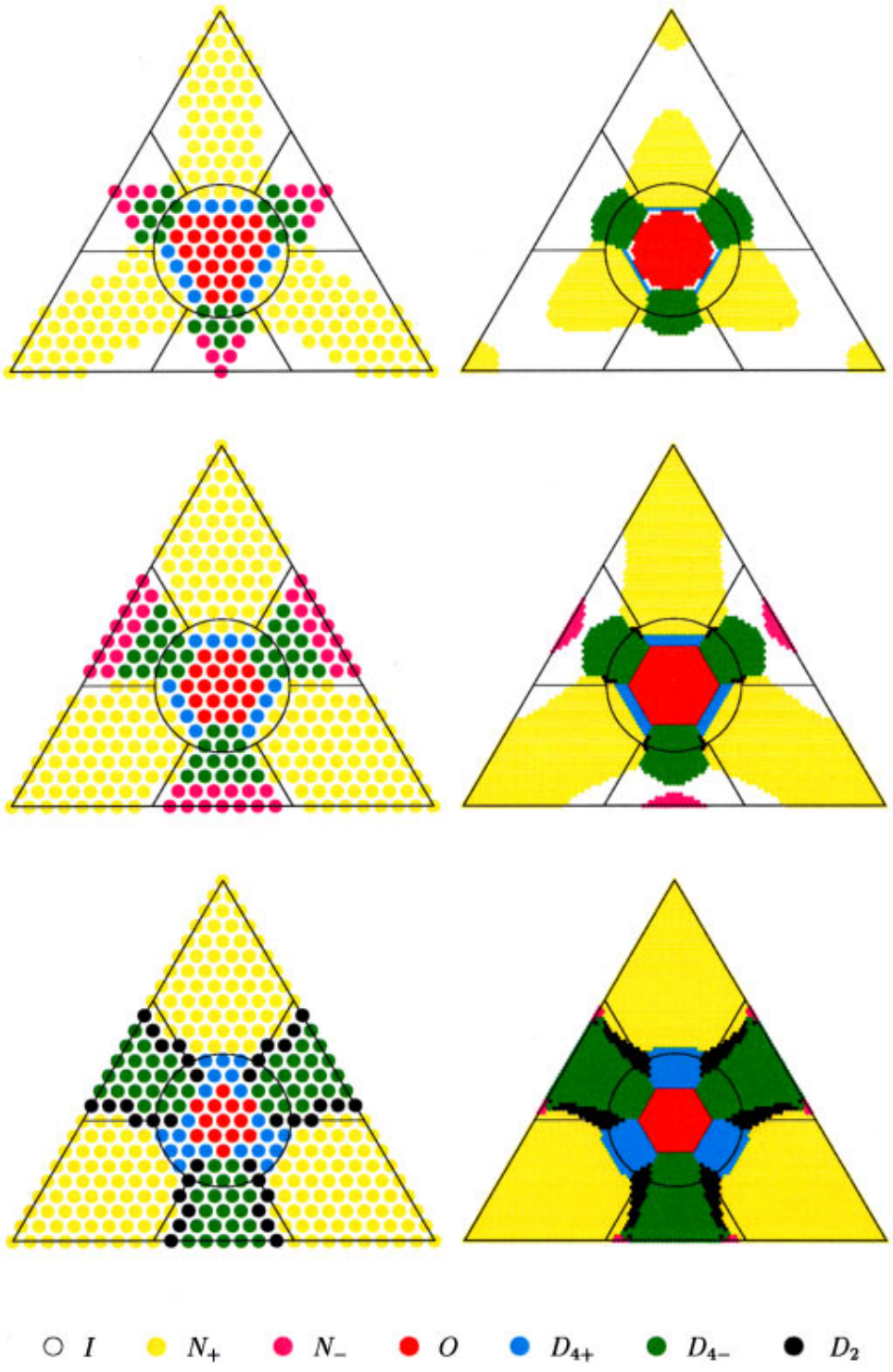

FIG. 3. (Color) Three constant density planes of the phase diagram. Diagrams on the left correspond to the minimization method, while those on the right to the Gaussian approximation. The lines correspond to the results obtained from the bifurcation theory. The scaled densities shown are, from top to bottom, $\eta/\eta_0 = 0.9$, 1.0, and 1.5. There are seven different phases: nematic ($N_\pm$), cubatic (O), biaxial (D_2), and D_4 ($D_{4\pm}$) phases. The subscript $+$ refers to a rodlike behavior and the subscript $-$ to a disklike behavior.

transition will take place, though the right phase is determined.

In Fig. 3, three cross sections of the phase diagram are depicted. They are drawn for rescaled densities $\eta/\eta_0 = 0.9$, 1.0, and 1.5. This scaling is used in order to compare the behavior of all particles around their densities of interest. This means, however, that due to the scaling the real density in the middle is almost 14 times as high as at the vertices of the triangle. Analogously to the distinction we made between a rodlike nematic N_+ and plateletlike nematic phase N_-, we do the same for the D_4 phase.

The lines represent the boundaries that we obtained from our bifurcation analysis and we see that they give a reasonable estimate of the real behavior. Around the points where a straight line meets an edge, we still find an isotropic phase at 90% of the bifurcation density. Though those regions become smaller when we approach the bifurcation density, it remains quite stable and it is possible that for a very small region there is a continuous transition. Due to the approximation of taking only functions with $l \leqslant 4$ into account, we cannot tell if it is. As far as we know, all other transitions are first order.

As expected, the nematic phase is found mainly outside the circle. However, there is a part of the rodlike nematic phase that extends into the circle and also in the regions where we expected a plateletlike behavior. Apparently the longest rod has a large influence on the system. The N_- phase is found only in small regions and since a platelet is a very crude approximation for these particles, it is not surprising that it remains unstable at high densities. It disappears at $\eta \approx 1.3\eta_0$ by going to the phase D_{4-} where there is a discrete orientational symmetry around the z axis.

Inside the circle, we could expect the nematic, the cubatic, and the D_4 phases. The cubatic phase is found in the middle for all particles that resemble the particle with three equal rods. It is surrounded by the D_4 phase.

If we increase the density, the D_2 phase appears along the boundaries between the phases for which the longest or shortest rod is ordered. It starts at a density of $\eta \approx 1.2\eta_0$, around the points where both D_4 phases and the N_+ phase meet each other, which is near the points where the straight lines and circle from the bifurcation analysis touch.

For very high densities, all particles with three rods of different length, end up in the D_2 phase in which rods with the same length are aligned. The particles for which two rods have the same length cannot go beyond the D_4 phase and they lay on the symmetry lines. The domains of the nematic and cubatic phase are merely points at the vertices and in the middle of the triangle.

C. Gaussian approximation

1. Nematic phase

We can obtain an approximate solution of the Onsager model describing the isotropic-nematic phase transition for long thin rods if we use the assumption that in the ordered phase the rods have a strongly peaked distribution around the z axis, which can be approximated by a Gaussian distribution. The same approximation can be used for the isotropic-cubatic transition for the symmetrical particle with three rods (see Ref. [21]).

It is possible to extend this approximation to our system for all phases. First we write the free energy

$$\beta f = \beta \hat{f} + \sigma(\alpha) + \eta\rho(\alpha), \tag{36}$$

where the first term is from the ideal noninteracting system, which is given by $\beta \hat{f} = \ln \eta + \text{const}$. The second part of the free energy describes the orientational entropy and is given by

$$\sigma(\alpha) = \int d\Omega\ \psi(\Omega) \ln[8\pi^2 \psi(\Omega)]. \tag{37}$$

The last term in the free energy is related to the translational entropy

$$\rho(\alpha) = \frac{4}{\pi} \int d\Omega \int d\Omega'\, \psi(\Omega)\psi(\Omega') \sum_{i,j}\ l_i l_j |\sin \gamma_{i,j}|. \tag{38}$$

In the isotropic phase, the ODF is a constant, $\psi(\Omega) = 1/8\pi^2$, which gives the exact results

$$\begin{aligned} \beta f_I &= \ln\eta + \eta, \\ \beta P_I &= (\eta + \eta^2)/\langle B_2 \rangle_I, \\ \beta \mu_I &= \ln\ \eta + 2\,\eta + 1. \end{aligned} \tag{39}$$

For a nematic phase where Ω is the direction of the ordering axis of particle, the factor $8\pi^2$ reduces to 4π. The trial function in the original Onsager model is given by

$$\psi(\Omega) = \frac{\alpha}{4\pi \sinh \alpha} \cosh(\alpha \cos\theta). \tag{40}$$

For large values of α this is a sharply peaked distribution with its main contribution around $\theta \approx 0$ and $\theta \approx \pi$, which we can approximate by Gaussians:

$$\begin{aligned} \psi(\Omega) &= \frac{\alpha}{4\pi} \exp\left(-\frac{1}{2}\alpha\theta^2 \right) \quad \left(0 \leqslant \theta \leqslant \frac{\pi}{2} \right), \\ \psi(\Omega) &= \frac{\alpha}{4\pi} \exp\left[-\frac{1}{2}\alpha(\theta - \pi)^2 \right] \quad \left(\frac{\pi}{2} \leqslant \theta \leqslant \pi \right). \end{aligned} \tag{41}$$

The orientational part of the entropy can easily be calculated in this approximation $\sigma(\alpha) = \ln(\alpha) - 1$. The translational part has three different type of contributions. The first is given by the interaction of the ordering rods which we label by l_3, and it is the longest one in case of a rodlike nematic phase and the shortest one in case of a plateletlike nematic phase

$$\rho_{3,3}(\alpha) \approx \frac{4l_3^2}{\sqrt{\pi\alpha}}. \tag{42}$$

This term is important for rodlike particles, while for plateletlike particles it is negligible. The second type is the interaction between one l_3 rod along the nematic axis and one that is perpendicular to it, for instance, l_1:

$$\rho_{1,3}(\alpha) \approx \frac{4l_1 l_3}{\pi}. \tag{43}$$

The last type consists of the interaction between two rods in the plane perpendicular to the nematic axis. Its main importance is for plateletlike particles. This contribution, however, is not properly described by the first term of the expansion if we use the Gaussian approximation, which is due to the fact that a typical value for α in this region is 12, too small for a qualitatively valid Gaussian approximation. For that reason, we use the original Onsager trial function to obtain a fit of this contribution, which we will denote by $J(\alpha)$:

$$\begin{aligned} \rho_{1,1}(\alpha) &\approx \frac{4l_1^2}{\pi} J(\alpha) \\ &= \frac{4l_1^2}{\pi}\left(0.639 + \frac{1.45}{\alpha} - \frac{12.3}{\alpha^2} + \frac{75.0}{\alpha^3} - \frac{178}{\alpha^4} \right). \end{aligned} \tag{44}$$

The total orientational entropy can now be written as

$$\rho(\alpha)=\frac{4l_3^2}{\sqrt{\pi\alpha}}+\frac{8}{\pi}l_3(1-l_3)+\frac{4}{\pi}(1-l_3)^2J(\alpha) \quad (45)$$

and depends only on the length of the ordering rod. Since the proper value for α should minimize the free energy we differentiate the expression with respect to α and equate it to zero:

$$\frac{d\beta f}{d\alpha}=\frac{1}{\alpha}-\eta\left(\frac{2l_3^2}{\alpha\sqrt{\alpha\pi}}-\frac{4}{\pi}(1-l_3)^2J'(\alpha)\right)=0. \quad (46)$$

Solving this equation results in the values of the pressure and chemical potential of the nematic phase for any density.

2. Cubatic phase

In order to describe the cubatic phase by a Gaussian distribution we switch over to the x,y,z convention of Eulerian axes. In this convention, the general rotation is given by three subsequent rotations around three perpendicular axes

$$\mathcal{D}(\Omega)=e^{-\imath\phi J_x}e^{-\imath\theta J_y}e^{-\imath\psi J_z}. \quad (47)$$

Thus, for the cubatic phase, we can use as a Gaussian-like distribution

$$\psi(\Omega)=\frac{1}{24}\left(\frac{\alpha}{2\pi}\right)^{3/2}\exp\left(-\frac{\alpha}{2}(\phi^2+\theta^2+\psi^2)\right). \quad (48)$$

There are 24 such contributions corresponding to 24 possible orientations for the particle to align with the three axes of the system. The orientational part is again easy to calculate and is given by

$$\sigma(\alpha)=\ln\left(\frac{8\pi^2}{24}\right)+\frac{3}{2}\ln\left(\frac{\alpha}{2\pi}\right)-\frac{3}{2}. \quad (49)$$

For the translational contribution to the free energy we have to add for all possible orientations the excluded volumes for the aligned and perpendicular pairs of rods, which gives

$$\rho(\alpha)=\frac{4}{3\sqrt{\pi\alpha}}+\frac{8}{3\pi}. \quad (50)$$

If we now minimize the expression for the free energy with respect to the parameter of the Gaussian α, we obtain

$$\alpha=\frac{16\eta^2}{81\pi}. \quad (51)$$

This gives us the free energy and hence the pressure and chemical potential of the cubatic phase in this approximation

$$\beta f_O=4\ln\eta+\ln\left[\frac{\pi^2}{3}\left(\frac{2\sqrt{2}}{9\pi}\right)^3\right]+\frac{3}{2}+\frac{8\eta}{3\pi},$$

$$\beta P_O=\left(4\eta+\frac{8}{3\pi}\eta^2\right)\Big/\langle B_2\rangle_I, \quad (52)$$

$$\beta\mu_O=4\ln\eta+\ln\left[\frac{\pi^2}{3}\left(\frac{2\sqrt{2}}{9\pi}\right)^3\right]+\frac{11}{2}+\frac{16\eta}{3\pi}.$$

If we combine these with the results for the isotropic phase (39), we obtain the coexisting densities η_I and η_O for the isotropic and cubatic phases, and the α parameter, describing the ordering strength of the cubatic phase at coexistence

$$\eta_I=48.43, \quad \eta_O=50.80, \quad \alpha=162.3. \quad (53)$$

This large value of α justifies the Gaussian approximation.

3. The D_4 and D_2 phases

In the case of a D_4 phase, there is one four-fold degenerate axis, which we take to be parallel to the z axis. Our trial function has now two parameters α and β. α describes the strength of ordering with respect to the z axis and β describes the strength of ordering with respect to the x and y axes, which are equivalent in this phase. The trial function has eight contributions of the form

$$\psi(\Omega)=\frac{1}{8}\left(\frac{\alpha^2\beta}{8\pi^3}\right)^{1/2}\exp\left(-\frac{1}{2}(\alpha\phi^2+\alpha^2\theta+\beta^2\psi^2)\right). \quad (54)$$

Again, we find a simple equation for σ:

$$\sigma(\alpha,\beta)=\ln\left(\frac{8\pi^2}{8}\right)+\frac{1}{2}\ln\left(\frac{\alpha^2\beta}{8\pi^3}\right)-\frac{3}{2}. \quad (55)$$

For ρ, however, we get an expression containing an elliptical integral of the second kind

$$\rho(\alpha,\beta)=\frac{4l_3^2}{\sqrt{\pi\alpha}}+\frac{4(1-l_3)^2}{\sqrt{\pi^3\beta}}E(\sqrt{1-\beta/\alpha})+\frac{2}{\pi}(1-l_3)(1+3l_3). \quad (56)$$

We minimize the free energy with respect to α and β. For $l_3>1/3$, this results in $\alpha>\beta$, which suggests a stronger ordering along the z direction, while for $l_3<1/3$ the opposite, $\beta>\alpha$, is found. Therefore, there is a stronger ordering along the x and y axes.

The treatment of the D_2 phase is similar to that of the D_4 phase, except that there are now only four possible orientations of the particle and we need three parameters in our trial function:

$$\psi(\Omega)=\frac{1}{4}\left(\frac{\alpha\beta\gamma}{8\pi^3}\right)^{1/2}\exp\left(-\frac{1}{2}(\alpha\phi^2+\beta^2\theta+\gamma^2\psi^2)\right). \quad (57)$$

There is a simple equation for σ, depending now on three parameters

$$\sigma(\alpha,\beta,\gamma)=\ln\left(\frac{8\pi^2}{4}\right)+\frac{1}{2}\ln\left(\frac{\alpha\beta\gamma}{8\pi^3}\right)-\frac{3}{2}, \quad (58)$$

and an expression for ρ, which is somewhat more complex

$$\rho(\alpha,\beta,\gamma)=\frac{8}{\pi^{3/2}}\left[\frac{l_3^2}{\sqrt{\beta}}E(\sqrt{1-\beta/\alpha})+\frac{l_2^2}{\sqrt{\gamma}}E(\sqrt{1-\gamma/\alpha})+\frac{l_1^2}{\sqrt{\gamma}}E(\sqrt{1-\gamma/\beta})\right]+\frac{4}{\pi}(1-r^2). \quad (59)$$

4. Results

If we combine the Gaussian approximations of the different phases we can calculate the coexistence by equating pressure and chemical potential. In Fig. 3 the phase diagram for several reduced density η/η_0 are depicted. In case the overall density, within our model, is not thermodynamically stable and hence leads to a phase separation, we have colored it to correspond to the most ordered phase.

At the density $\eta/\eta_0=1$ we have shown the isotropic phase to be unstable, but there are still isotropic areas. This artifact is a consequence of our model: The assumption of strongly peaked distributions is not valid here. Furthermore, we find that the boundaries between the cubatic and D_4 phases are straight lines. This seems somewhat surprising but is merely a consequence of losing particle information in the approximation. This can be seen from the expression for the free energy, which depends only on the length of one rod, corresponding to the main axis of the particle. The only difference for these particles is due to a different scaling because η_0 also depends on the same rod length, but this effect is too small to be visible here. Some areas are very tiny and cannot be seen in the diagram at all. For instance, between the cubatic and D_4 phases of both types there is a narrow strip of particles that have at this density coexistence between the cubatic and D_2 phases.

It is not observed and intuitively also not expected that there are particles that go from rodlike to plateletlike behavior, for instance, via a transition from the N_- to a D_{4+} phase. Also, a phase transition from a cubatic phase to a nematic phase, and thus to a phase with higher symmetry, is not found. All data confirmed that phase transitions in this model can only go to lower symmetries, i.e., a transition from the isotropic phase to either a nematic or a cubatic phase, followed by a transition to the D_4 and finally the D_2 phase, although one or more phases can, in principle, be surpassed.

In Fig. 4 we have plotted a cross section of the phase diagram along the symmetry line $l_1=l_2$, where we multiplied the density with B_2, the isotropic second virial coefficient. Since these particles are four-fold symmetric around the l_3 rod, they cannot go beyond the D_4 phase in which they all will end up with only two exceptions, the cubatic particle and the single rod particle. As was explained before, the N_- phase is very unstable and is found only in a very small region and will for somewhat higher densities already form a D_4 phase. The N_+ phase is much more stable. The isotropic-cubatic phase transition takes place at a density that is almost 14 times as high as the isotropic-nematic phase transition for the single rod.

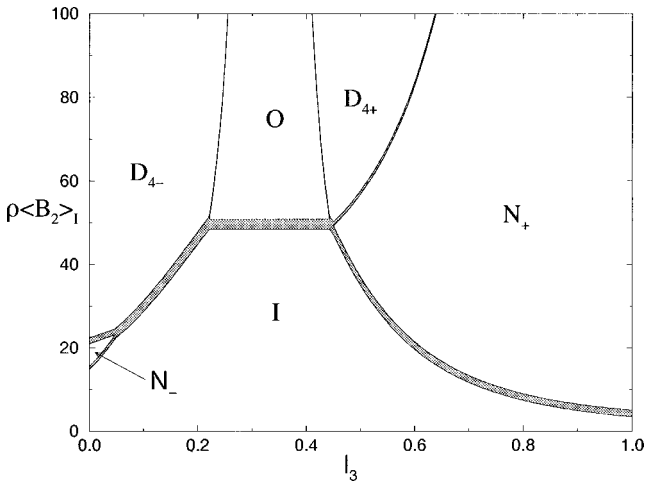

FIG. 4. Cross section of the phase diagram along the symmetry line ($l_1=l_2$) of the density vs the length of the remaining rod.

IV. CONCLUSIONS

We have shown that the phase behavior of crosslike particles is surprisingly rich. Within a single phase diagram, we find, apart from the well-known rodlike and platelike nematic phases N_+ and N_-, the more elusive biaxial nematic phase, here denoted as D_2, as well as the nematic phase with a fourfold axis D_4 and the cubatic phase O. With respect to the original suggestion for the cubatic phase, it is noteworthy that our analysis predicts that at intermediate densities this phase could be realized even for particles that themselves do not possess perfect O_h symmetry. Even in the Onsager approximation the necessary calculations are not trivial, however, as all three orientational degrees of freedom need to be taken into account. We have shown that bifurcation analysis provides an effective tool to determine some of the important properties of the phase diagram, at least in the density regime where the isotropic phase becomes unstable. The higher-density regime requires much more work. Fortunately, our results show that the generalized Gaussian approximation is quite reliable in this regime, thus allowing the phase diagram to be approximated without unduly expensive calculations.

Of course, we need to pose the question whether our results obtained in the Onsager limit have any bearing on the behavior of particles with finite aspect ratio parts at nonzero packing fractions. To this end, both the validity of the Onsager approximation itself, i.e., is it justified to neglect the third and higher virial contributions, and our retention of only the leading term in the pair excluded volume (4) have to be checked. Preliminary results [30] from direct evaluations of the relevant Mayer diagrams in the isotropic phase, indicate that the rods should have unrealistic aspect ratios of order 10^3 for these assumptions to hold. Perhaps a more important barrier to the formation of the phases described here are posed by kinetic effects. The amount of interdigitation of these crosslike particles even at relatively low packing fractions is so high that these systems might very well form orientational glasses rather than phases with long-range orientational order. A hint of this behavior was found in Monte Carlo (MC) simulations we performed in a system with crosslike particles composed of three equally long spherocylinders of aspect ratio 25 [31]. In spite of a simula-

tion technique specially geared towards effectively sampling the phase space of glassy systems (pressure hopping MC which is a variant of Hamiltonian hopping MC [32]), we were not able to obtain an orientationally ordered phase. A way out of this problem and at the same time a possible experimental realization of a cubatic was suggested to us by Jullien [33]: Do not use particles with a fixed shape, but rather particles that can self-assemble into the required shape. In this case the kinetic barriers may be circumvented by the continuous disassociation and reassociation of the parts. Examples of such systems that could in principle be synthesized are cube-shaped organometallic complexes to which elongated ligands can attach in a reversible manner.

ACKNOWLEDGMENTS

We thank James Polson and Martin Bates for a critical reading of the manuscript. The work of the FOM Institute is part of the research program of FOM and is made possible by financial support from the Netherlands Organization for Scientific Research (NWO).

APPENDIX: PROPERTIES OF THE Δ FUNCTIONS

In order to derive the symmetry adapted Δ functions as defined by Eq. (9), we make use of properties of the Wigner matrices $\mathcal{D}^l_{m,n}(\Omega)$ as can be found in [23]. By reasons of symmetry l has an integral value and the indices m and n are integers in the region $-l,\ldots l$.

If we take the definition of our Δ functions (7), use the closure relation $\mathcal{D}^l_{m,n}(\Omega_1\Omega_2)=\Sigma^l_{p=-l}\mathcal{D}^l_{m,p}(\Omega_1)\mathcal{D}^l_{p,n}(\Omega_2)$, and rearrange the summations we obtain

$$\Delta^l_{m,n}(\Omega)=\frac{1}{\sqrt{N}}\sum_{p,q}\left(\sum_{g'\in D_2}\mathcal{D}^l_{m,p}(g')\right)\times\mathcal{D}^l_{p,q}(\Omega)\left(\sum_{g\in D_2}\mathcal{D}^l_{q,n}(g^{-1})\right). \tag{A1}$$

Note that the elements of the group D_2 are their own inverse. The summations over the elements of D_2 can be done explicitly and are nonzero only if both m and n are even. This leads to the final form (9) of the symmetry adapted functions. The normalization follows from distinguishing zero and nonzero values for m and n.

Since $\mathcal{D}^l_{m,n}(\Omega^{-1})=\mathcal{D}^l_{n,m}(\Omega)^*$ and $\mathcal{D}^l_{m,n}(\Omega)^*=(-1)^{m-n}\mathcal{D}^l_{-m,-n}(\Omega)$, the Δ functions are real valued and satisfy

$$\Delta^l_{m,n}(\Omega^{-1})=\Delta^l_{n,m}(\Omega). \tag{A2}$$

It is clear that we cannot find a closure relation on the set of Δ functions. The reason is simply that a general rotation will always break the symmetry of the group D_2 and hence introduce functions that are outside the set of Δ functions. There is, however, a restricted set of rotations that leave our space of functions invariant. This set consists of the elements of the cubic group O. In order to prove this we only need to show that this is true for two generators of this group, which are the rotations over an angle $\pi/2$ about the z axis (R_z) and the y axis (R_y). It is not difficult to prove that for both rotations R_z and R_y

$$\Delta^l_{m,n}(\Omega R)=\sum_{p\ \text{even}\geqslant 0}\Delta^l_{m,p}(\Omega)\Delta^l_{p,n}(R), \tag{A3}$$

$$\Delta^l_{m,n}(R\Omega)=\sum_{p\ \text{even}\geqslant 0}\Delta^l_{m,p}(R)\Delta^l_{p,n}(\Omega). \tag{A4}$$

This will automatically be valid for all combinations of these two rotations and hence for all elements R of the cubic group O.

In Eq. (19) we have defined a functional on our space of real valued functions. If we first apply this definition directly on the complex valued rotation matrix elements we obtain

$$\mathcal{D}^l_{m,n}[\mathcal{D}^{l'}_{m',n'}](\Omega)=\int d\Omega'\,\mathcal{D}^l_{m,n}(\Omega'^{-1}\Omega)\mathcal{D}^{l'}_{m',n'}(\Omega'). \tag{A5}$$

Using the closure relation and the properties for an inverse rotation, the integral over Ω' results in

$$\mathcal{D}^l_{m,n}[\mathcal{D}^{l'}_{m',n'}]=\frac{8\pi^2}{2l+1}\delta_{l,l'}\delta_{m,n'}\mathcal{D}^l_{m',n}. \tag{A6}$$

It is now a simple matter of checking that if we do the same thing for the Δ functions this leads directly to

$$\Delta^l_{m,n}[\Delta^{l'}_{m',n'}]=\frac{8\pi^2}{2l+1}\delta_{l,l'}\delta_{m,n'}\Delta^l_{m',n}. \tag{A7}$$

Finally we show the result for an the integral over three Δ functions. Again, the only way to obtain this result is by distinguishing the different combinations of zero and nonzero indices

$$\int\Delta^l_{m,n}(\Omega)\Delta^{l'}_{m',n'}(\Omega)\Delta^{l''}_{m'',n''}(\Omega)d\Omega=8\pi^2\left(\frac{1}{2}\sqrt{2}\right)^{2-\delta_{0,mm'm''}-\delta_{0,mm'm''}}\times\begin{pmatrix}l & l' & l''\\ m & \sigma'm' & \sigma''m''\end{pmatrix}\begin{pmatrix}l & l' & l''\\ n & \tau'n' & \tau''n''\end{pmatrix}, \tag{A8}$$

where the matrices denote Wigner 3-j symbols and $\sigma',\sigma'',\tau',\tau''$ are ±1 and chosen in such a way that $m+\sigma'm'+\sigma''m''=n+\tau'n'+\tau''n''=0$. There is only one possible restriction to this formula: In the case $m=0$ or $n=0$ the σ's or τ's are not uniquely defined. This causes the 3-j symbols to differ if and only if $l+l'+l''$ is an odd integer, in which case the sign changes. To avoid this one should if possible choose the m and n to be nonzero by taking a suitable permutation of the Δ functions.

[1] M. J. Freiser, Phys. Rev. Lett. **24**, 1041 (1970).
[2] R. Alben, Phys. Rev. Lett. **30**, 778 (1973).
[3] J. P. Straley, Phys. Rev. A **10**, 1881 (1974).
[4] B. Mulder, Phys. Rev. A **39**, 360 (1989).
[5] R. Holyst and A. Poniewierski, Mol. Phys. **69**, 193 (1990).
[6] A. Ferrarini, P. L. Nordio, E. Spolaore, and G. R. Luckhurst, J. Chem. Soc., Faraday Trans. **91**, 3177 (1995).
[7] Y. Rabin, W. E. McMullen, and W. M. Gelbart, Mol. Cryst. Liq. Cryst. **89**, 67 (1982).
[8] Z. Y. Chen and J. M. Deutch, J. Chem. Phys. **80**, 2151 (1983).
[9] R. G. Caflish, Z. Y. Chen, A. N. Berker, and J. M. Deutch, Phys. Rev. A **30**, 2562 (1982).
[10] A. Stroobants and H. N. W. Lekkerkerker, J. Chem. Phys. **88**, 3669 (1984).
[11] M. P. Allen, Liq. Cryst. **8**, 499 (1990).
[12] P. J. Camp and M. P. Allen, J. Chem. Phys. **106**, 6681 (1997).
[13] S. Sarman, J. Chem. Phys. **104**, 342 (1996).
[14] J. Malthête, L. Liébert, A. M. Levelut, and Y. Galerne, C. R. Acad. Sci. Paris **303**, 1073 (1986).
[15] S. Chandrasekhar, B. K. Sadashiva, S. Ramesha, and B. S. Srikanta, Pramana **27**, L713 (1988).
[16] S. Chandrasekhar, B. R. Ratna, B. K. Sadashiva, and V. N. Raja, Mol. Cryst. Liq. Cryst. **165**, 123 (1988).
[17] S. Chandrasekhar, V. N. Raja, and B. K. Sadashiva, Mol. Cryst. Liq. Cryst., Lett. Sect. **7**, 65 (1990).
[18] K. Praefcke, B. Kohne, B. Gündogan, D. Singer, D. Demus, S. Diele, G. Pelzl, and U. Bakowsky, Mol. Cryst. Liq. Cryst. **198**, 393 (1991).
[19] J. F. Li, V. Percec, C. Rosenblatt, and O. D. Lavrentovich, Europhys. Lett. **25**, 199 (1994).
[20] S. M. Fan, I. D. Fletcher, B. Gündogan, N. J. Heaton, G. Kothe, G. R. Luckhurst, and K. Praefcke, Chem. Phys. Lett. **204**, 517 (1993).
[21] D. Frenkel, in *Liquids, Freezing and Glass Transition*, edited by J. P. Hansen, D. Levesque, and J. Zinn-Justin (North-Holland, Amsterdam, 1991), pp. 689–762.
[22] L. Onsager, Ann. (N.Y.) Acad. Sci. **51**, 627 (1949).
[23] D. M. Brink and G. R. Satchler, *Angular Momentum*, 2nd ed. (Oxford University Press, Oxford, 1968).
[24] M. Fialkowski, A. Kapanowski, and K. Sokalski, Mol. Cryst. Liq. Cryst. Sci. Technol., Sect. A **265**, 371 (1995).
[25] I. S. Gradshteyn and I. M. Ryzhik, *Table of Integrals, Series, and Products*, 5th ed. (Academic, San Diego, 1994).
[26] R. F. Kayser and H. J. Raveché, Phys. Rev. A **17**, 2067 (1978).
[27] J. A. C. Veerman and D. Frenkel, Phys. Rev. A **45**, 5632 (1992).
[28] R. Blaak, Ph.D. thesis, University of Utrecht, 1997 (unpublished).
[29] M. Hamermesh, *Group Theory*, 2nd ed. (Addison-Wesley, Reading, MA, 1964).
[30] R. Blaak and B. M. Mulder, Mol. Phys. **94**, 401 (1998).
[31] R. Blaak, D. Frenkel, and B. M. Mulder (unpublished).
[32] C. J. Geyer, in *Proceedings of the 23rd Symposium on the Interface* (American Statistaical Association, New York, 1991), pp. 156–163.
[33] L. Jullien (private communication).